as AxCANCre, AxCALacZ, was also purchased from Riken Gene Bank as a control vector.
14. Ninety percent hepatectomy was done by removing the median, left lateral, right upper, and lower lobes by ligation, leaving only the caudate lobe. After surgery, animals were allowed free access to tap water supplemented with 10% dextrose and received a daily intravenous injection of 2 ml of saline.
15. For intrasplenic transplantation, a small surgical incision was made in the animal's flank, and the spleen was exposed under anesthesia and surgical care approved by the animal committee of Okayama University Medical School. Cells (50×10^6) suspended in 0.5 ml of ASF-104 were injected into the inferior pole of the spleen. The blood flow in the splenic artery and vein was temporarily occluded to avoid immediate passage of cells into the portal vein during transplantation. The injection site was also ligated to prevent cell leakage and bleeding.
16. Blood samples were obtained from tail veins, and the levels of T.Bil, PT, and NH3 were measured with Fuji Dry Chem (Tokyo, Japan).
17. N. Kobayashi *et al.*, data not shown.
18. Spleen specimens were compound embedded and frozen at −80°C. Cryostat sections of the spleen (5-μm thick) were fixed in ice-cold acetone. Immunofluorescence for SV40T of NKNT-3 cells transplanted into the spleen was performed as the same procedure as described in (*11*).
19. M. Gossen *et al.*, *Science* **268**, 1766 (1995).
20. R. Pawliuk *et al.*, *Nature Med.* **5**, 768 (1999).
21. NKNT-3 cells (6×10^6) were plated in T75 flasks and infected 1 day later with AxCANCre at various MOI for 1 hour. Cells were subsequently cultured in the chemically defined serum-free medium ASF-104 (Ajinomoto, Tokyo, Japan) for 2 days and then harvested for RT-PCR, Western blot, and Northern blot analyses.
22. Infection of AxCANCre was performed as described in (*21*). After adenoviral infection, NKNT-3 cells were cultured in ASF-104 medium containing G418 (500 μg/ml) for 7 days and then harvested for RT-PCR, Western blot, and Northern blot analyses.
23. Total RNA was isolated by the RNAzol procedure (Cinna/BioTecx, Friendswood, TX). RT was performed at 22°C for 10 min and then 42°C for 20 min with 1 μg of RNA per reaction. PCR was performed with specific primers in volumes of 50 μl and according to the manufacturer's instructions (PCR kit; Perkin-Elmer/Cetus, Norwalk, CT). Primers used were as follows: for SV40T, 5′ primer CAGGCATAGAGTGTCTGC and 3′ primer CAACAGCCTGTTGGCATATG; and for β-actin, 5′ primer TGACGGGGTCACCCACACTGTGCCCATCTA and 3′ primer CTAGAAGCATTTGCGGTGGACGATGGAGGG. PCR conditions were as follows: denaturation at 92°C for 1 min, annealing at 58°C for 1 min, and elongation at 72°C for 1 min with a thermal cycler (Perkin-Elmer, Foster City, CA). PCR products were resolved on 2% agarose gels and visualized by ethidium bromide staining.
24. Proteins (30 μg per lane) from NKNT-3 cells and reverted NKNT-3 cells were separated by electrophoresis on SDS-polyacrylamide gels, transferred to hybond–polyvinylidene difluoride transfer membranes, and treated with mouse monoclonal antibody to SV40T (Santa Cruz Biotechnology) (1:100) followed by peroxidase-linked secondary antibody (1:2500). Labeled protein bands were stained with ECL kit (Amersham, Japan). Human β-actin protein served as an internal control.
25. Northern blot analysis was performed as described (*3*). Specific DNA probes were obtained by PCR of genomic DNA and then radiolabeled.
26. We thank J. Miyazaki for providing the CAG promoter and H. Lodish and I. M. London for comments on the manuscript. Supported by NIH grants HL55435 to P.L. and DK48794 to I.J.F.

4 November 1999; accepted 23 December 1999

The Glucocorticoid Receptor: Rapid Exchange with Regulatory Sites in Living Cells

James G. McNally,* Waltraud G. Müller,* Dawn Walker, Ronald Wolford, Gordon L. Hager†

Steroid receptors bind to site-specific response elements in chromatin and modulate gene expression in a hormone-dependent fashion. With the use of a tandem array of mouse mammary tumor virus reporter elements and a form of glucocorticoid receptor labeled with green fluorescent protein, targeting of the receptor to response elements in live mouse cells was observed. Photobleaching experiments provide direct evidence that the hormone-occupied receptor undergoes rapid exchange between chromatin and the nucleoplasmic compartment. Thus, the interaction of regulatory proteins with target sites in chromatin is a more dynamic process than previously believed.

Steroid receptors modulate rates of transcription at target genes through protein-protein interactions with basal transcription factors and through the recruitment of a variety of coactivators or corepressors (*1*). Some of these interacting proteins serve as bridging factors to other components of the soluble transcription apparatus, and others either harbor intrinsic chromatin-modifying activities [such as acetylation or methylation (*2*)] or interact with other chromatin-remodeling activities [including the swi/snf family of nucleosome-remodeling proteins (*3*)]. The dynamic process by which the receptors recruit these factors to activate transcription is poorly understood. The classic view is that the receptor binds to a recognition site and remains at that site for as long as the ligand is present in the cellular milieu (*4*). Alternatively, the receptor may interact transiently with a response element, recruiting a secondary set of factors that in turn form a stable complex at the regulatory site. This type of mechanism has been referred to as "hit and run" and has been proposed both for the glucocorticoid receptor (GR) (*5*, *6*) and for enhancer function in general (*7*) (Fig. 1). These issues could not be addressed by the indirect methods traditionally used to detect transcription factor– DNA binding and function. We report here the direct observation of GR interaction with hormone response elements in living cells. Using photobleaching techniques, we show that the receptor undergoes continuous exchange between chromatin regulatory elements and the nucleoplasmic compartment when ligand is constantly available.

The cell line 3134 contains a large tandem array of a mouse mammary tumor virus/Harvey viral ras (MMTV/v-Ha-ras) reporter (*8*). The repeat structure arose from the spontaneous chromosomal integration of a 9-kb bovine papilloma virus (BPV) multicopy episome, creating a head-to-tail array of 1.8×10^6 base pairs (bp) (Fig. 2A). This structure contains about 200 copies of the long terminal repeat (LTR) and thus includes 800 to 1200 binding sites for GR. Derivatives of this cell line express a green fluorescent protein (GFP)–tagged version of GR (GFP-GR) from a chromosomal locus under control of the tetracycline-repressible promoter (*8*). The GFP-GR that is expressed in these cell lines after removal of tetracycline is resident in the cytoplasm in the absence of ligand but translocates to the nucleus within 10 min of hormone addition, as detected by live-cell epifluorescence (*8*).

The MMTV array in these cell lines was large enough to be observed by light microscopy. Fluorescence in situ hybridization analysis (FISH) of DNA was performed on metaphase chromosomes from cell line 3617 with a probe to the ras insert in the tandem array (Fig. 2). The cell line is aneuploid, as expected for a ras-transformed murine carcinoma cell maintained in culture for many generations. Hybridization with the ras probe alone revealed the presence of a large ras-specific structure near the centromere of one chromosome (Fig. 2C). Subsequent analysis with a chromosome 4 telomere-specific probe showed that the array was located on this chromosome (Fig. 2B). The array thus exists as a unique amplified element near the centromere in the A region of chromosome 4 (Fig. 2A).

When the distribution of GFP-GR is examined in living cells (Fig. 3), multiple nuclear structures are observed after ligand activation (*9*). The receptor is located in a series of bright focal structures, overlayed against a fine reticular pattern that is present throughout the nucleus but not including the nucleoli. In cell line 3617, however, the receptor also accumulates in one large structure that is present as one copy

Laboratory of Receptor Biology and Gene Expression, Building 41, Room B602, National Cancer Institute, Bethesda, MD 20892–5055, USA.

*These authors contributed equally to this work.
†To whom correspondence should be addressed. E-mail: hagerg@exchange.nih.gov

per nucleus (Fig. 3A). In a representative experiment, this unique structure was observed in 66% of cells examined (*10*). Nuclei from two adjacent cells in one field are shown in Fig. 3, B and C; one bright object is present in each nucleus.

We carried out in situ RNA hybridization to detect nascent transcripts homologous to the MMTV-ras array and detected a large structure similar in size to that observed with GFP-GR in the nuclei of 3617 cells (Fig. 4A; compare with Fig. 4C). Merged images for the GFP-GR fluorescence-labeled and rhodamine-labeled nucleic acid probe (Fig. 4B) indicated that the GFP-GR structure present at one copy per nucleus was directly associated with nascent transcripts from the amplified MMTV LTR array. These results provide definitive evidence that targeting of GFP-GR to the LTR hormone response elements has been detected (*11*).

The observed association of ligand-activated GR with the MMTV promoter for observable periods of time is consistent with either the static (Fig. 1, model 1) or the hit-and-run model (Fig. 1, model 2). To distinguish between these models, we performed two types of photobleaching experiments that detect the mobility of molecules in living cells, fluorescence recovery after photobleaching (FRAP) (*12*) and fluorescence loss in photobleaching (FLIP) (*13*) (Fig. 5). In FRAP mode (*12*), a focused laser beam was used to exclusively bleach GFP-GR on the array (Fig. 5, A to F). After irradiation, GFP-GR was rapidly replaced with unbleached molecules. In FLIP mode (*13*), GFP-GR elsewhere in the nucleus was continuously bleached (Fig. 5, G to O). During irradiation, GFP-GR on the array was replaced with nonfluorescent molecules from the nucleoplasmic space, either endogenous GR or bleached GFP-GR, or both. Thus, GFP-GR exchanges at a high rate between the array bound state and the free nucleoplasmic state. This result is consistent only with model 2 of Fig. 1; that is, GFP-GR cycles continuously on and off the MMTV chromatin target in hormone-stimulated cells.

During the GR-induced chromatin transition in the MMTV LTR, secondary transcription factors including NF 1 and Oct 1 bind to the B/A nucleosome region after receptor activa-

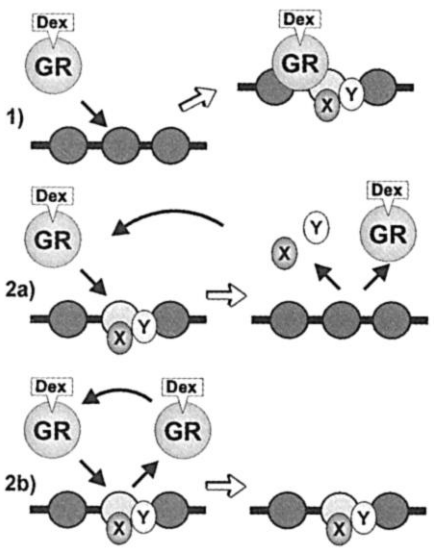

Fig. 1. Models for the dynamic interaction of GR with the MMTV locus, depicting the binding of GR to a chromatin fiber. Model 1 indicates static binding of GR to the target locus. Model 2 postulates recycling (hit-and-run) mechanisms, either for GR alone (2b) or for both GR and secondary factors (x, y) (2a) that bind in response to the chromatin transition. Dex, dexamethasone.

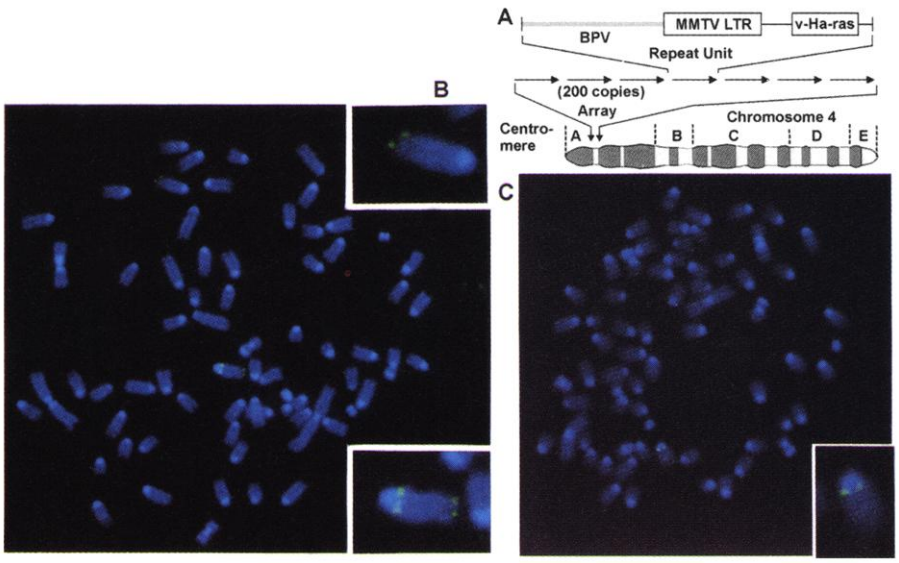

Fig. 2. A 200-copy MMTV LTR array is located on chromosome 4. Cell line 3617 contains a large-scale tandem array of the MMTV LTR (*7*). The array contains about 200 copies of an MMTV-LTR-ras-BPV reporter structure in a perfect head-to-tail array of 1.8×10^6 bp (*8*) (**A**); the structure thus contains 800 to 1200 binding sites for GR. The chromosomal location of the array was determined by metaphase FISH analysis of DNA with a 565-bp fluorescein-conjugated probe specific to the v-ras sequences [chromosomes are 4,6-diamidino-2-phenylindole (DAPI) stained]. (**C**) A metaphase spread of the 3617 cells with one region of strong hybridization on two sister chromatids (inset). The metaphase figure in (**B**) was hybridized with both the ras probe and a chromosome 4 telomere-specific probe (Genome Systems, St. Louis, MO). Two copies of chromosome 4 are detected in the figure: the LTR array is present on one copy (bottom inset) and absent on the second (top inset), indicating that the array is integrated near the centromere of chromosome 4 (A).

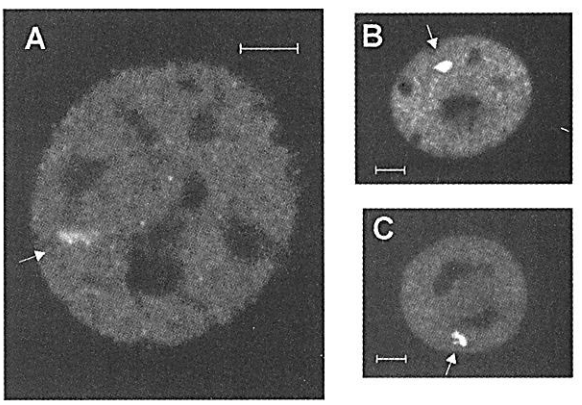

Fig. 3. GFP-GR binding to the MMTV LTR in living cells. 3617 cells (*8*) were grown in Dulbecco's modified Eagle's medium (DMEM) (Gibco BRL, Grand Island, NY) supplemented with 10% fetal bovine serum (HyClone, Logan, UT) in the presence of tetracycline (5 μg/ml). For GFP-GR imaging, cells were transferred either to 22-mm-square cover slips resting in wells of a six-well plate or to self-enclosed chambered cover slips (Nalge Nunc International, Naperville, IL). At the time of transfer, the medium was replaced with DMEM without tetracycline (to induce GFP-GR expression) and supplemented with 10% charcoal-dextran–treated serum (to prevent hormone stimulation of the GFP-GR). After 16 to 24 hours, dexamethasone was added to the cells to induce nuclear accumulation of the GFP-GR. After 2 hours of dexamethasone treatment, cells were imaged with a 100×/1.4 numerical aperture oil immersion lens on a Leica TCS NT SP laser scanning confocal microscope. GFP was excited with the 488-nm line from an argon laser. The confocal pinhole was set at 1.0 Airy disk unit. (**A**) A two-dimensional (2D) section showing a representative nucleus after 2-hour induction with 5 nM dexamethasone. Arrow indicates the array. (**B** and **C**) Projections of 3D images of two nuclei from the same field, each showing a single array structure (arrows) after 2-hour treatment with 1 nM dexamethasone. Scale bars, 5 μm.

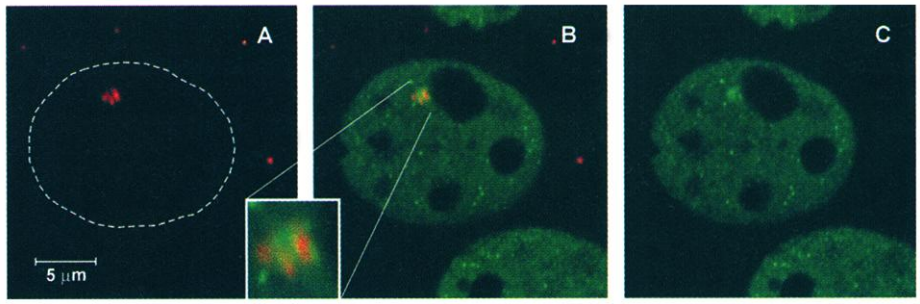

Fig. 4. Colocalization of GFP-GR with nascent MMTV transcripts detected by RNA FISH. Cells were grown as described in Fig. 3. Dexamethasone at 100 nM was added for 12 min; cells were then fixed for 15 min in 3.5% paraformaldehyde and washed three times for 10 min each with phosphate-buffered saline (PBS). The fixed cells were permeablized with 0.5% Triton X-100 in PBS for 10 min, and then washed again three times for 10 min in PBS, followed by a 5-min rinse in 2× saline sodium citrate (SSC). Cover slips were then incubated for 18 hours at 37°C with 20 μl of hybridization mixture [containing 2× SSC, 50% formamide, 10% dextran sulfate, tRNA (1 mg/ml), and probe DNA (5 to 10 μg/ml)]. Probe DNA was prepared with a biotin nick-translation kit (Boehringer, Indianapolis, IN) and plasmid pM18, which includes the MMTV LTR, v-ras and BPV (*19*). The nick-translated DNA was denatured in formamide at 95°C for 10 min and then placed on ice for 5 min before addition to the hybridization mixture. After hybridization, cover slips were washed for 15 min in 2× SSC and 0.05% Triton X-100 and washed again for 15 min in 2× SSC and then for 5 min in 4× SSC. Cover slips were incubated for 1 hour in avidin-rhodamine (2 μg/ml) in 4× SSC, 0.1% bovine serum albumin and 0.01% Tween 20, then washed once for 10 min in 4× SSC containing 0.05% Triton X-100, and twice for 10 min in 4× SSC, followed by one rinse in PBS. Cover slips were then mounted on a slide for viewing by confocal microscopy as described in Fig 2. Rhodamine fluorescence (**A**) was detected with the 568-nm Kryton laser line. GFP-GR fluorescence is shown in (**C**), and merged images are shown in (**B**). Scale bar = 5 μm.

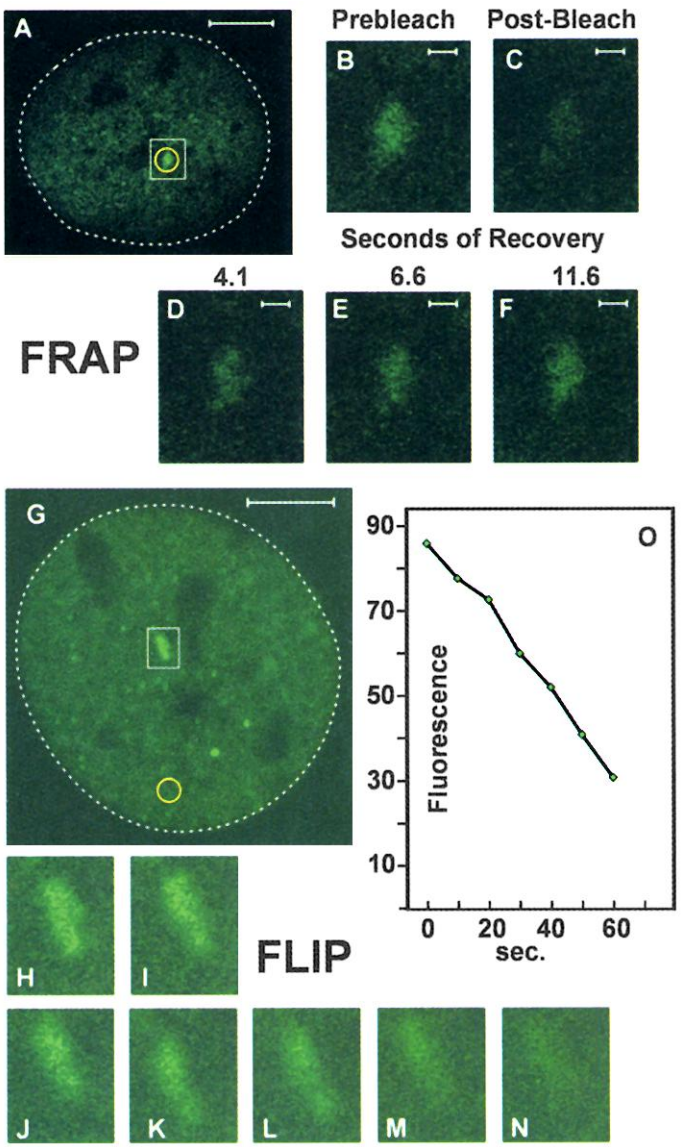

Fig. 5. GFP-GR undergoes rapid exchange with the LTR in the continuous presence of ligand. (**A** to **F**) GFP-GR bound to the LTR array was subjected to FRAP (*12*). Cells were grown and imaged as described in Figs. 3 and 4. The time-lapse/bleach mode was used on the Leica TCS NT SP confocal microscope. Settings were configured to produce a prebleach image (A) first and then focus a 1.5-μm diameter beam (indicated by yellow circle) on the array with the 488- and 514-nm lines of the argon laser for 0.25 s. The first postbleach image was collected at 1.6 s [(C) corresponds to the white box in (A)], followed by images collected at 2.5-s intervals. Here, the 4.1-s (D), 6.6-s (E), and 11.6-s (F) images are shown. Leica-supplied software was used to quantify fluorescence recovery. The cell shown here was treated with 1 μM dexamethasone for 2.5 hours and kept at 37°C during imaging. (A), scale bar, 5 μm. (B to F) scale bars = 0.5 μm. (**G** to **O**) Nuclear GFP-GR was subjected to FLIP (*13*). A 1.5-μm diameter beam was focused within the nucleus at a distance from the array [indicated by yellow circle, (G)], and irradiation carried out repetitively as follows: 1 s beam on, 1 s beam off, 1.6 s low intensity, full-frame image collection. Images of the array [corresponding to the white box in (G)] are shown in (H) to (N) for 0, 10, 20, 30, 40, 50, and 60 s after initiation of FLIP. Relative intensities for fluorescence associated with the array are presented in (O). Scale bar in (G), 5 μm.

tion and are continuously detected on the promoter by exonuclease footprinting analysis (*6*, *14*). One role of the secondary factors could be to maintain the open chromatin structure (Fig. 1, model 2b). The footprinting data, together with our observations, suggest two pathways for assembly of the GR-induced complex. Chromatin may cycle very rapidly between the "open," enzyme-accessible, and "closed" states, coincident with the exchange observed for GFP-GR (Fig. 1, model 2a). Alternatively, GR may induce a long-lived open state through the recruitment of remodeling activities and secondary transcription factors, but the continuous presence of GR is unnecessary to maintain this state (Fig. 1, model 2b). In vitro results with reconstituted MMTV LTR chromatin are consistent with the hit-and-run mechanism. Purified GR bound to nucleosome B in MMTV chromatin restricts access to B-region enzyme sites; however, access is enhanced by addition of adenosine triphosphate (ATP) and a chromatin-remodeling fraction (*15*). Thus, it appears that ATP-dependent remodeling by GR in this in vitro system is accompanied by receptor disengagement from the template.

Although some components of the large transcriptional apparatus may cycle through the complex (*16*), it is generally assumed that a stable initiation complex exists under conditions where the primary activator remains competent (Fig. 1, model 1). We suggest a more dynamic view. The detection of a long-lived footprint, or hypersensitive transition, does not verify continuous occupancy of a regulatory site but rather indicates an equilibrium in favor of the occupied state at the time. Assaying occupancy usually involves processes such as cell disruption, isolation of nuclei, and chromatin extraction, all of which are conditions that would interrupt the dynamic process of exchange. Using FRAP in living cells, Ellenberg and colleagues (*17*) have shown that GFP-labeled histone H2B does not exchange from general euchromatic sites. In contrast, we have

measured rapid exchange rates for a transcription factor on a specific regulatory element in living cells. It is unclear whether any of the various factors recruited to a regulatory site remain statically bound.

The continuous exchange of liganded receptor with genomic targets is likely to have important consequences for physiologic responses of the cell. Many receptor responses are modulated by multiple cellular signaling pathways. For example, phosphorylation events mediated through independent protein kinase cascades can quickly alter the receptor-mediated expression level at a variety of promoters. Rapid exchange of a nuclear receptor with regulatory sites may facilitate the action of these secondary pathways because the receptor would be continuously available for modification, even in the presence of ligand.

The success of these experiments now opens the possibility of studying the direct interaction of many receptor coactivators and other receptor interaction activities with a natural gene target in real time in living cells. Further enhancements of this approach will likely lead to the ability to directly study molecular interactions at target regulatory regions through the application of fluorescent energy transfer (*18*) and proximity imaging of GFP-labeled factors (*18*).

References and Notes

1. H. Gronemeyer, in *Steroid Hormone Action*, M. G. Parker, Ed. (Oxford Univ. Press, New York, 1993), p. 94; M. G. Parker, *Curr. Opin. Cell Biol.* **5**, 499 (1993); N. J. McKenna, R. B. Lanz, B. W. O'Malley, *Endocr. Rev.* **20**, 321 (1999); L. Xu, C. K. Glass, M. G. Rosenfeld, *Curr. Opin. Genet. Dev.* **9**, 140 (1999).
2. T. E. Spencer *et al.*, *Nature* **389**, 194 (1997); C. A. Hassig, T. C. Fleischer, A. N. Billin, S. L. Schreiber, D. E. Ayer, *Cell* **89**, 341 (1997); D. Chen *et al.*, *Science* **284**, 2174 (1999).
3. C. Muchardt and M. Yaniv, *EMBO J.* **12**, 4279 (1993); S. K. Yoshinaga, C. L. Peterson, I. Herskowitz, K. R. Yamamoto, *Science* **258**, 1598 (1992); H. Chiba, M. Muramatsu, A. Nomoto, H. Kato, *Nucleic Acids Res.* **22**, 1815 (1994); C. J. Fryer and T. K. Archer, *Nature* **393**, 88 (1998).
4. P. Becker, R. Renkawitz, G. Schutz, *EMBO J.* **3**, 2015 (1984).
5. G. Rigaud, J. Roux, R. Pictet, T. Grange, *Cell* **67**, 977 (1991).
6. M. Truss, G. Chalepakis, M. Beato, *J. Steroid Biochem. Mol. Biol.* **43**, 365 (1992).
7. C. S. Suen *et al.*, *J. Biol. Chem.* **273**, 27645 (1998).
8. D. Walker, H. Htun, G. L. Hager, *Methods* **19**, 386 (1999); P. Kramer *et al.*, *J. Biol. Chem.* **274**, 28590 (1999).
9. G. L. Hager, in *Green Fluorescent Protein*, vol. 302 of *Methods in Enzymology*, M. P. Conn, Ed. (Academic Press, San Diego, CA, 1999), p. 73; H. Htun, J. Barsony, I. Renyi, D. J. Gould, G. L. Hager, *Proc. Natl. Acad. Sci. U.S.A.* **93**, 4845 (1996).
10. The 3617 cell line is aneuploid and chromosome 4 varies in copy number, even in the haploid state. Thus, some of the cells in the population may not score for the LTR array because they are missing that copy of chromosome 4.
11. A. Belmont and colleagues [C. C. Robinett *et al.*, *J. Cell Biol.* **135**, 1685 (1996)] developed a system in which a GFP-tagged lac repressor was shown to bind highly amplified copies of the lac operator element that was integrated in the chromosomes of CHO cells. They have used that system to study chromosome dynamics during the cell cycle. Others [I. Carmi, J. B. Kopczynski, B. J. Meyer, *Nature* **396**, 168 (1998)] have detected the interaction of transcription factors with amplified binding sites through immunofluorescence. A strength of the approach described here is that it uses an intact mammalian promoter with no alteration of the promoter and its associated regulatory elements. A somewhat surprising finding is that the density of GR-binding sites in the 3617 array is sufficiently high to permit easy detection of GFP-GR binding to the response elements. The arrays described by Belmont and colleagues contain a simple, highly reiterated lac operator sequence with a density of binding sites about two orders of magnitude higher than used here.
12. FRAP experiments (Fig. 5, A to F) were carried out as follows. A beam of light using the 488- and 514-nm laser lines was focused on the tandem array structure (Fig. 5A) in live cells after hormone stimulation. After a bleach pulse of 0.25 s, almost all GFP-GR molecules associated with the array structure had been bleached (Fig. 5, B and C). When irradiation of the structure was discontinued, GFP-GR fluorescence was again detected in association with the array structure within 2 s. There is a minimum 1.6-s delay between the end of the bleaching pulse and acquisition of the first image on the Leica confocal instrument (Exton, PA). Thus, the first image collected immediately after bleaching (Fig. 5C) is actually 1.6 s after bleaching. The very small amount of GFP-GR visualized in this image probably represents rebinding in this first 1.6-s period.
13. For FLIP experiments (Fig. 5, G to O), the 488- and 514-nm laser line beam of light was focused in the nucleus of living, hormone-treated cells at a distance from the position of the MMTV array (Fig. 5G). After collecting an initial complete image of the nucleus, the distant position was repeatedly irradiated as follows: 1 s of irradiation was followed by 1 s with no light, and then a full nuclear image was recorded with low-intensity excitation. This regimen was repeated for a total elasped time of 1 to 2 min.
14. H. Richard-Foy and G. L. Hager, *EMBO J.* **6**, 2321 (1987); M. G. Cordingley, A. T. Riegel, G. L. Hager, *Cell* **48**, 261 (1987); T. K. Archer, P. Lefebvre, R. G. Wolford, G. L. Hager, *Science* **255**, 1573 (1992); G. Fragoso, S. John, M. S. Roberts, G. L. Hager, *Genes Dev.* **9**, 1933 (1995); G. Fragoso and G. L. Hager, *Methods* **11**, 246 (1997); C. L. Smith and G. L. Hager, *J. Biol. Chem.* **272**, 27493 (1997); G. Fragoso, W. D. Pennie, S. John, G. L. Hager, *Mol. Cell. Biol.* **18**, 3633 (1998).
15. T. M. Fletcher *et al.*, in preparation.
16. S. Hahn, *Cell* **95**, 579 (1998); A. J. Berk, *Curr. Opin. Cell Biol.* **11**, 330 (1999).
17. J. Ellenberg, in preparation.
18. R. Heim and R. Y. Tsien, *Curr. Biol.* **6**, 178 (1996); D. A. De Angelis, G. Miesenbock, B. V. Zemelman, J. E. Rothman, *Proc. Natl. Acad. Sci. U.S.A.* **95**, 12312 (1998).
19. M. C. Ostrowski, H. Richard-Foy, R. G. Wolford, D. S. Berard, G. L. Hager, *Mol. Cell. Biol.* **3**, 2045 (1983).

16 November 1999; accepted 21 December 1999

Dopaminergic Loss and Inclusion Body Formation in α-Synuclein Mice: Implications for Neurodegenerative Disorders

Eliezer Masliah,[1,2]* Edward Rockenstein,[1] Isaac Veinbergs,[2] Margaret Mallory,[1] Makoto Hashimoto,[1] Ayako Takeda,[1,3] Yutaka Sagara,[2] Abbyann Sisk,[2] Lennart Mucke[4]

To elucidate the role of the synaptic protein α-synuclein in neurodegenerative disorders, transgenic mice expressing wild-type human α-synuclein were generated. Neuronal expression of human α-synuclein resulted in progressive accumulation of α-synuclein—and ubiquitin-immunoreactive inclusions in neurons in the neocortex, hippocampus, and substantia nigra. Ultrastructural analysis revealed both electron-dense intranuclear deposits and cytoplasmic inclusions. These alterations were associated with loss of dopaminergic terminals in the basal ganglia and with motor impairments. These results suggest that accumulation of wild-type α-synuclein may play a causal role in Parkinson's disease and related conditions.

Human α-synuclein is a 140–amino acid molecule (*1*) that is encoded by a gene on chromosome 4 (*2*) and has homology to rat and *Torpedo* α-synuclein and songbird synelfin (*3*). Although the precise function of the synuclein superfamily of peptides is still unknown, several lines of evidence suggest potential roles in synaptic function and neural plasticity (*3*, *4*). Human α-synuclein was originally isolated from plaques of Alzheimer's disease brains as a 19-kD protein precursor of the highly hydrophobic 35–amino acid metabolite, nonamyloid component (NAC) of plaques (*1*). The NAC peptide can self-aggregate into fibrils and induces aggregation of the β-amyloid peptide (*5*). α-Synuclein is highly abundant in presynaptic terminals (*4*) and in Lewy bodies (*6*), neuronal inclusions that are found in diverse human neurodegenerative disorders including the Lewy body variant of Alzheimer's disease, diffuse Lewy body disease, and Parkinson's disease (*7*). Rare cases of familial Parkinson's disease have recently been linked to point mutations in α-synuclein (*8*); however, most neurodegenerative disorders with Lewy bodies are associated with abnormal accumulation of wild-type, not mutant, α-synuclein (*6*, *9*).

To elucidate the role of α-synuclein accumulation in the pathogenesis of neurodegenerative disorders with Lewy bodies, we generated